Available online at www.sciencedirect.com
ScienceDirect
Journal of Power Sources 171 (2007) 86–91
JOURNAL OF POWER SOURCES
www.elsevier.com/locate/jpowsour

Short communication

Formation and evaluation of semi-IPN of nafion 117 membrane for direct methanol fuel cell
1. Crosslinked sulfonated polystyrene in the pores of nafion 117

P.P. Kundu [1], Beom Taek Kim, Ji Eun Ahn, Hak Soo Han, Yong Gun Shul *

Department of Chemical Engineering, Yonsei University, 134 Sinchon Dong, Seodaemun-gu, Seoul 120-749, Republic of Korea

Received 3 October 2006; accepted 27 October 2006
Available online 8 December 2006

Abstract

The in situ polymerization and crosslinking of sodium salt of sulfonated styrene in the pores of nafion 117 membrane has been studied for the evaluation of electrical performance of the resultant semi-IPN (semi-interpenetrating polymer network) membrane in direct methanol fuel cell (DMFC). The formation of semi-IPN is confirmed from the presence of aromatic characteristics peak in the FTIR spectra. Impedance results indicate that the semi-IPN sample with higher water uptake exhibits lower interfacial resistance compared to a sample with water uptake. This indicates that the semi-IPN formed in the pores of nafion 117 membrane has the ability to reduce methanol crossover by blocking the transportation. At higher temperatures (>110 °C) and lower current density (<25 mA cm^{-2}), the electrical performance (power density) of a DMFC with a representative semi-IPN sample is observed to be higher than that with a nafion membrane.

Keywords: DMFC; Semi-IPN; Methanol crossover; Power density

1. Introduction

Fuel cells are electrochemical devices to generate electricity [1]. In direct methanol fuel cell (DMFC), the methanol fuel is fed directly into the cell for its oxidation and subsequent generation of protons in the anode [2,3]. Currently, worldwide research is focused on designing direct oxidation fuel cell systems for small applications [4,5]. DMFC power system has several advantages for providing power to a car [6,7] and small electrical gadgets [8,9]. Firstly, methanol is abundantly available and to some extent biorenewable. It is easy handling and of high energy content, thus providing a compact means of storing energy. DMFC power systems are also environmentally friendly. The anodic oxidation of aqueous methanol in a DMFC yields carbon dioxide and protons. The generated protons pass through a proton-conductive, electronically non-conductive membrane.

Nafion was tried for the use as proton conducting membranes in DMFC [10,11]. The main problem encountered in using nafion as membrane in DMFC is the low electrical output compared to the conventional hydrogen fed fuel cells. The low output is caused by the anodic catalyst deactivation by the generated carbon monoxide and methanol crossover through the membrane [12,13]. Methanol crossover is a phenomenon whereby methanol molecules pass from the anode to the cathode side of the membrane. Cross or reverse potential is also generated when the "crossed over" methanol is oxidized in the cathode chamber. Methanol crossover occurs because present membrane electrolytes are permeable (to some degree) to methanol and water [14–16].

Methanol crossover can be reduced by the blocking the channels through the pores of the membranes by some methanol repelling species [17–25]. Another way of reducing methanol crossover is the reduction of methanol concentration in the membrane region by increasing anodic catalytic oxidation. This can be done by an increase in the electrochemical reaction temperature [26]. At higher temperature (say 110 °C), the anodic chamber becomes less humidified and the dimensional stability of nafion is almost disrupted. All these cause the nafion less

* Corresponding author. Tel.: +82 2 2123 2758; fax: +82 2 312 6401.
E-mail addresses: ppk923@yahoo.com (P.P. Kundu), shulyg@yonsei.ac.kr (Y.G. Shul).
[1] On vacation from the Department of Chemical Technology, SLIET, Longowal 148106, India.

0378-7753/$ – see front matter © 2006 Elsevier B.V. All rights reserved.
doi:10.1016/j.jpowsour.2006.10.099

proton conductive at higher temperature. As the generated protons in the anode are conducted through the aqueous phase, the increased water uptake of the membrane may help in efficient proton conduction. Keeping in view of these objectives, several authors tried to modify the nafion membrane by grafting comonomers on the nafion [17,18] and by forming in situ nanocomposites [19–24]. It has been reported that the formation of semi-IPN of poly (APTS) with nafion membrane, it is possible to improve the performance [25].

Both of nafion and methanol are polar aliphatic chains and they may have some affinity. To reduce that affinity, it is hypothesized that some aromatic components inside the pores of nafion may reduce the methanol crossover. With the idea of improving the performance of DMFC, the present work aimed to prepare semi-IPN of sulfonated polystyrene in the pores of nafion membrane by means of impregnation and subsequent in situ polymerization and crosslinking.

2. Experimental

2.1. Materials used

Nafion 117 membrane (thickness 175 μm) purchased from DuPont was used after immersion in DI water for 24 h. Sodium salt of sulfonated styrene (SS), divinyl benzene (DVB), 2,2′-azobisisobytronitrile (AIBN), dimethyl formamide (DMF) were purchased from Aldrich and used as received. The chemical structure of monomer (SS), crosslinker (DVB), initiator (AIBN) and nafion are depicted in Fig. 1.

2.2. Preparation of semi-IPN

For the preparation of semi-IPN, the reactants were mixed as per the compositions in Table 1. The weighted nafion membrane was soaked overnight at room temperature in 50 ml of DMF under magnetic stirring. The other reactants as in Table 1 were added with continued stirring for 24 h to allow complete impregnation of the reactants along with the solvent (DMF) throughout the pores of nafion. The whole mixture was heated for two hours at 90 °C. During heating, the impregnated SS was in situ polymerized and crosslinked in the pores of nafion to form a semi-IPN. At the end of reaction, the rest of crosslinked SS was separated out from the DMF solution as a precipitate. The semi-IPN of nafion membrane was transferred to a beaker containing 100 ml of 3:7 H_2SO_4 and water mixture. For proper protonation of sodium salt of sulfonated polystyrene, the semi-IPN of nafion membrane was treated with a 50:50 H_2SO_4 and water mixture for 12 h. The protonated semi-IPN of nafion membrane was then dried under vacuum at 80 °C for 24 h.

Table 1
Compositions of comonomer (SS) and crosslinker (DVB) used for the formation of semi-interpenetrating polymer network of nafion 117 membrane

Comonomer/ crosslinker	Compositions of the samples used for impregnation of nafion 117 membrane (g g^{-1} of nafion 117)			
	Sample A	Sample B	Sample C	Sample D
SS	2.0	1.0	4.0	2.0
DVB	0.04	0.02	0.08	0.08
AIBN	0.02	0.01	0.04	0.02

SS: sodium salt of sulfonated styrene; DVB: divinyl benzene; AIBN: 2,2′-azobisisobyronitrile.

2.3. Characterization of semi-IPN of nafion 117

2.3.1. Water uptake of membrane

A piece of vacuum dried sample was weighed and put in a beaker containing DI water for 24 h for its proper soaking with water. On taking the sample out of the beaker, the excess water on the surface of the membrane was wiped out. Then, it was weighed for its wet weight. The water uptake was calculated as

$$\text{water uptake}\,(\%) = 100 \times \frac{w_{\text{wet}} - w_{\text{dry}}}{w_{\text{dry}}} \quad (1)$$

where w_{wet} and w_{dry} are the weights of wet and dry samples, respectively.

2.3.2. Change in membrane thickness on water absorption

The thickness of a vacuum dried sample was measured with a thickness gauge. The sample was placed in DI water for 24 h for proper soaking. The thickness of the wet sample was measured

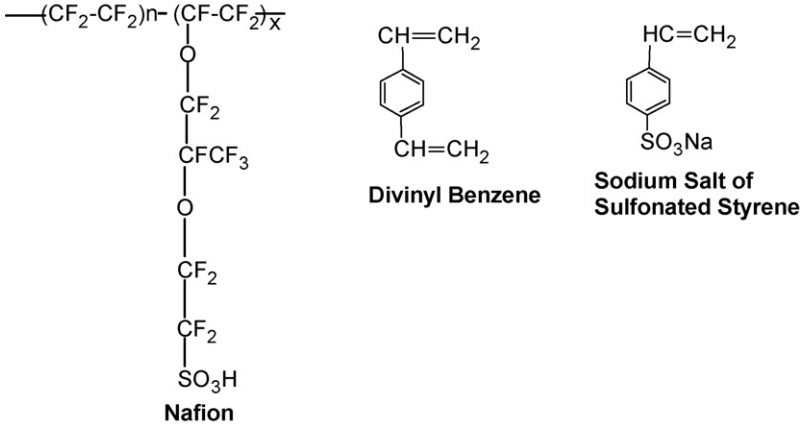

Fig. 1. Chemical structure of nafion, divinylbenzne and sodium salt of sulfonated styrene.

carefully. The change in thickness of the membrane on water absorption was calculated as

$$\text{change in thickness}\,(\%) = 100 \times \frac{T_{\text{wet}} - T_{\text{dry}}}{T_{\text{dry}}} \quad (2)$$

where T_{wet} and T_{dry} are the thickness of wet and dry samples, respectively.

2.3.3. Fourier transform Infrared (FTIR)–attenuated total reflectance (ATR) spectroscopy

A FTIR spectroscope (Genesis series of ATI Mattson Co.) equipped with a DTGS detector and a flat plate ATR sampling accessory was used to obtain the IR spectra of the membranes. A thallium/iodide (KRS-5) parallelogram crystal with an angle of incident of 45° was employed. All of the ATR spectra were collected at 4 cm^{-1} resolution, with 32 scans being accumulated for each sample. Three sets of spectra were recorded for each sample and were found to be identical.

2.3.4. Fabrication of membrane-electrode assembly (MEA)

A catalyst mixture containing 40% of carbon (VCXC72 of E-TeK) and 60 wt% of Pt–Ru (30:30:40 Pt:Ru:C for anode) or Pt (60:40 Pt:C for cathode) were magnetically stirred with isopropanol and 5 wt% nafion solution (of DuPont). Sonication and stirring was repeated for several times and stirring continued for 24 h at room temperature. At the end, a fine ink of catalyst was prepared. The ink was carefully sprayed on the membrane such that uniform thickness of catalyst was maintained throughout the membrane surface. The metal catalyst (Pt) loading was 4 mg cm^{-2}. The electrodes were dried at 80 °C for 2 h. A Teflon sheet of 250 μm thickness was used as gasket. The spray coated membrane, gaskets and front and back side plates were hot pressed (1.5 t) at 125 °C for 6 min for getting final membrane–electrode assembly.

2.3.5. ac impedance spectroscopy

An impedance analyzer (Autolab FRA) was used to measure the changes in membrane interface resistance. During testing, the anode and cathode was used as a reference and a working electrode, respectively. In the frequency range of 100 mHz to 100 kHz, the response to the ac amplitude of 0.05 V was measured.

2.3.6. DMFC cell performance

A 2 M aqueous solution of methanol was pumped to the anode at a flow rate of 50–60 ml min^{-1}. Pure oxygen was flown to the cathode at a rate of 40 ml min^{-1}. A dc electronic load (Hewlett Packard 6060 B) was used to measure the voltage of the MEA. Current was measured with a micro-elctronic device (Keithley 2000).

3. Results and discussions

The water uptake and change in thickness on the absorption of water calculated from Eqs. (1) and (2), respectively, are plotted as bar diagram in Fig. 2. All the samples have higher water uptake values than that of nafion. It was reported

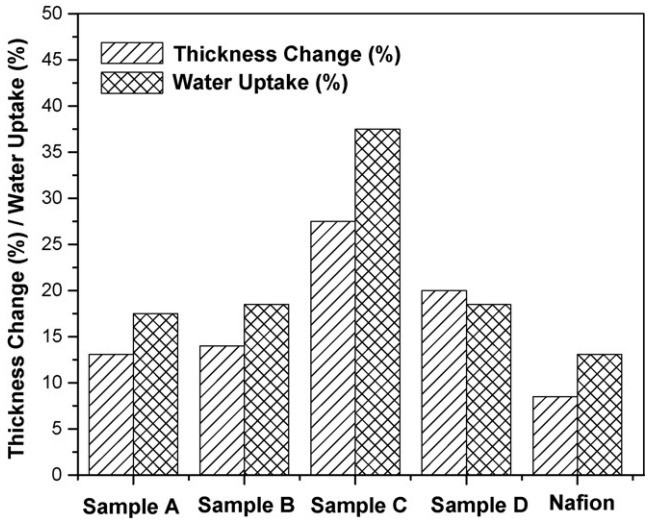

Fig. 2. Change of thickness (%) and water uptake (%) of samples on swelling in the water.

elsewhere that when 2-acrylamido-2-methyl-1-propane sulfonic acid was in situ polymerized in the pores of nafion, the water uptake of semi-IPN nafion membranes were reduced to a lower value [25]. The reason of reduced water uptake was cited as the blockage of the nafion pores by the formation of semi-IPN. By the same reasoning, it is expected that the formation of semi-IPN of nafion by the in situ polymerization of sulfonated styrene (SS) should reduce the water uptake of the nafion. The results are just contrary to the expectation (Fig. 2). The sulfonic acid group attached to the benzene ring is more acidic than the one which is attached with aliphatic chain. The higher acidic and more polar sulfonated polystyrene attracts more water than 2-acrylamido-2-methyl-1-propane sulfonic acid. Due to the higher water attracting power of sulfonated polystyrene, one interconnected water channel forms inside the pores of the nafion and exhibits higher water uptake on the formation of semi-IPN.

Fig. 2 also reveals that with increase in SS content, water uptake value increases. Thus, sample C prepared from higher SS content (see Table 1) shows the maximum water uptake. Sample D prepared from a composition, which has similar SS content as that of sample B. The only difference between them is the higher crosslinker (DVB) content in D. From Fig. 2, the higher water uptake in D indicates that the crosslinker has significant effect on the water uptake.

From Fig. 2, the change in thickness on water absorption is observed to exhibit a similar pattern as that of water uptake. The changing pattern in the thickness change of the IPN membranes with change in SS content can be explained in a similar fashion as that of water uptake.

The FTIR–ATR spectra of the samples are shown in Fig. 3. The characteristics peaks at 1202 and 1142 cm^{-1} in nafion and nafion-based semi-IPNs are due to the C–H stretching vibrations of the PTFE backbone. The peaks at around 970 and 1055 cm^{-1} arise from the stretching vibrations of S–O and C–H bonds, respectively [17]. The peak at 1681 cm^{-1} is present in all of the semi-IPNs but not observed in nafion. This peak is assigned to

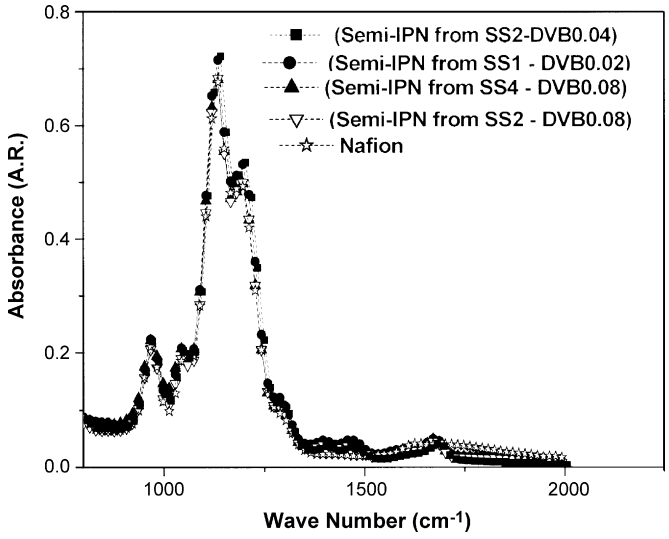

Fig. 3. FTIR absorbance spectra of the samples.

the C=C stretching vibrations of the aromatic benzene ring of sufonated polystyrene [17].

The imaginary and real part of impedance across the membranes is plotted in Fig. 4. From the Nesquist impedance plots, it is observed that the interfacial resistance for nafion is a minimum, followed by the samples C, D, A and B. The generated protons in anode chamber are transported across the membrane along with water. Therefore, an increase in proton conductivity and hence a decrease in interfacial resistance is expected with an increase in water uptake. Thus, according to the water uptake results (Fig. 2), sample C and nafion should exhibit the lowest and the highest resistance, respectively. This apparent paradox can be explained by considering all possible factors for imparting the interfacial resistance such as thickness and water affinity of the membrane, and the generated reverse potential of hydrogen ions due to cathodic oxidation of crossed over methanol. The increased water uptake on the formation of semi IPN of nafion allows easy transportation of methanol along with water through the membrane. Thus, keeping in view of only crossed methanol factor, nafion is expectedly showing lower resistance.

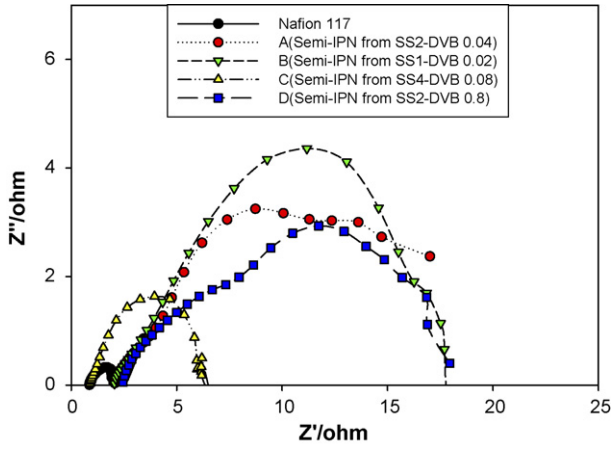

Fig. 4. Variation of real and imaginary impedance for the semi-IPN samples and nafion at 80 °C.

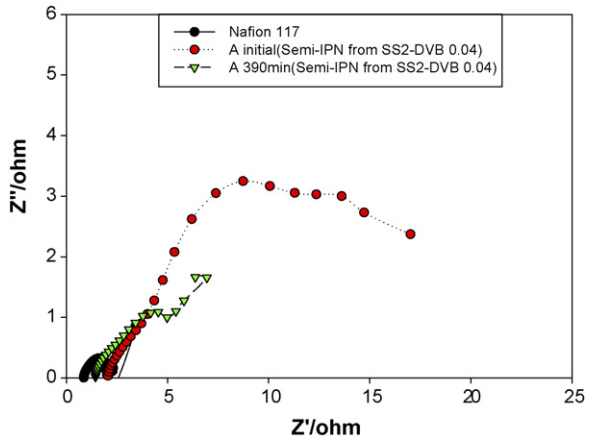

Fig. 5. Comparison of impedance results for nafion and sample A (semi-IPN from SS2-DVB0.04) tested after initialization and after 390 min.

On the other hand, sample C with the highest water uptake and change in thickness (%) is expected to exhibit the highest resistance as far as the methanol cross over factor is concerned. But, as in Fig. 4, it shows a minimum resistance amongst the semi-IPNs. This indicates that the semi-IPN formation in the pores of nafion has reasonable methanol blocking capability.

Fig. 5 shows comparison of impedance results of sample A, which was tested at two different time intervals. The sample A tested after 390 min of initialization shows much lower resistance compared to the initial one. The impedance of the sample A after 390 min approaches that of nafion, tested just after initialization. The reason for reduced interfacial resistance after prolonged time may be due to the effective participation of anodic catalysts for generation of hydrogen ions. The generated hydrogen ions in the immediate neighborhood of water molecules associate to form hydronium ions (H_3O^+). The hydronium ions forces sulfonic acid groups of the polymer membrane to dissociate to its fullest extent after prolonged time. This causes the effective transportation of hydronium ions through the membrane leading to reduce interfacial resistance of the membrane. We have tested only sample A after prolonged time. For all other samples, a similar behavior is expected.

Fig. 6 shows the impedance results for sample A at various temperatures. As temperature increases from 80 to 150 °C, the interfacial resistance across the membrane increases. According to Gibb's thermodynamic equation, the rate of overall electrochemical reaction should increase with the temperature. This should impose on faster rate of transportation of protons through the membranes leading to lowering of interfacial resistance. But, actually as in Fig. 6, the observed increase may be explained by the decreased retention of water by the membrane at higher temperature (>90 °C) [16,26]. The generated protons in the anode become mobile through hydronium ions. The anhydrous nature of the membrane causes disruption of transportation of protons.

The DMFC cell performance at 80 °C using various membranes is measured by the characteristics plots of potential and current density in Fig. 7. The performance of a cell is measured as power density from the area under the plot of potential versus current density. It is observed that the performances of the

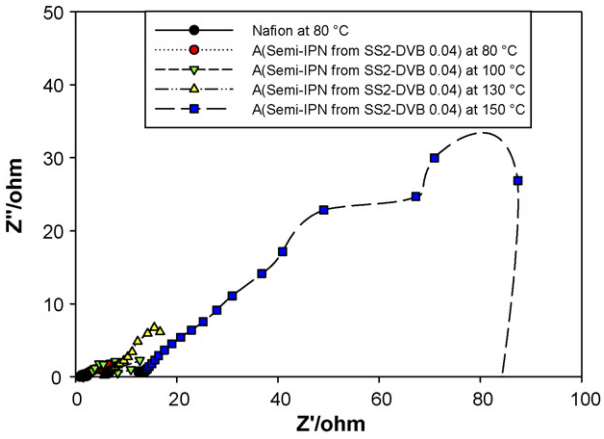

Fig. 6. Comparison of impedance of nafion at 60 °C with that of sample A (semi-IPN from SS2-DVB0.04) at 80, 100, 130 and 150 °C.

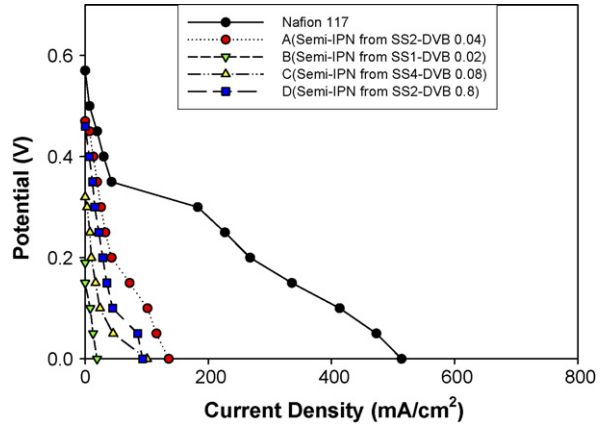

Fig. 7. Plots of potential versus current density for the measurement of DMFC cell performance using semi-IPN samples and nafion as membrane at 80 °C.

all the semi-IPN membranes are lower that that for nafion 117. This is due to the increased interfacial resistance of the semi-IPN membranes originated from the increased methanol crossover.

The effect of testing DMFC performance after prolonged time is depicted in Fig. 8. The cell performance using semi-IPN

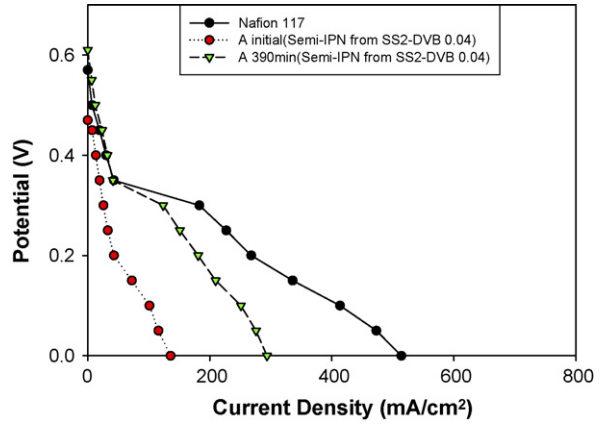

Fig. 8. Comparison of DMFC cell performance by using a membrane of nafion and sample A (semi-IPN from SS2-DVB0.04) and performance were tested after initialization and after 390 min.

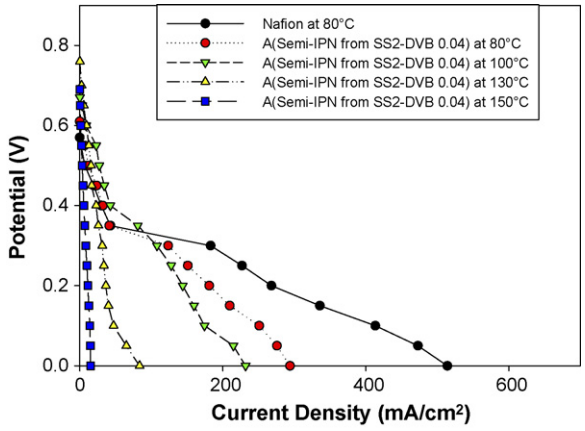

Fig. 9. Comparison of DMFC cell performance with nafion membrane at 60 °C and the sample A (semi-IPN from SS2-DVB0.04) at 80, 100, 130 and 150 °C.

membrane (sample A) at 80 °C is considerably improved after 390 min. After prolonged time from initialization, the catalytic effect for anodic oxidation reaches optimum. This imposes the maximization of electrolytic behavior of the membrane, leading to better transportation of protons and hence better cell performance is observed.

The effect of cell temperature on the DMFC performance is examined for sample A in Fig. 9. The overall cell performance is diminished with an increase in the temperature. But, the open circuit voltage (OCV) is increased with temperature up to 130 °C, beyond which it decreases. At 150 °C, the membrane A loses its dimensional stability leading to exhibit a low performance as well as an OCV. It was reported elsewhere that the performance of nafion at higher temperature (>110 °C, the glass transition temperature of nafion) is negligible [16]. Thus, the results for nafion at higher temperature (>80 °C) are not shown in Fig. 9. It is also observed in Fig. 9 that at low current density (<25 mA cm^{-2}), the performance of the cell with membrane A increases with increase in temperature up to 130 °C. The performance of the cell with membrane A at a higher temperature and at a low current density is even better than that for nafion at 80 °C. The formation of semi-IPN of sulfonated polystyrene inside the pores of nafion membrane increases the water uptake of the membranes (Fig. 2). This permits better interconnection between sulfonium anions of the membrane and the transported hydronuim ions. Thus, at high temperature, the anhydrous nature of nafion is diminished to a considerable extent by the formation of semi-IPN in the pores. This results in better DMFC performance at a low current density (<25 mA cm^{-2}) at a higher temperature.

4. Conclusion

The semi-IPN of sodium salt of sulfonated styrene (SS) is formed by the in situ polymerization and crosslinking in the pores of nafion 117 membrane. This is confirmed from the FTIR spectroscopy as well as from the water uptake results. The impedance results indicate that the semi-IPN of SS in the pores of nafion has reasonable blocking capability of methanol, lead-

ing to the reduction in methanol crossover. Hence, in contrary to the expectation from the water uptake results, less interfacial resistance is observed in sample C compared to the semi-IPNs. At higher temperatures (>110 °C) and at lower current densities (<25 mA cm^{-2}), the DMFC performance in terms of power density with a representative semi-IPN membrane (sample A) is vastly improved compared to that with a nafion 117 membrane. The open circuit voltage (OCV) of the DMFC with a semi-IPN membrane increases with an increase in temperature. This is due to the blocking effect of methanol (causing reduction in methanol crossover) as well as reducing anhydrous condition of the membrane at higher temperature by the formation of semi-IPN of SS in the pores of nafion.

Acknowledgement

One of the authors (PPK) appreciates the financial assistance from Korea Research Foundation (KRF 2005-005-J01402).

References

[1] J. Larminie, A. Dicks, Fuel Cell Systems Explained, 2nd ed., John Wiley & Sons, West Sussex, UK, 2003, pp. 1–14.
[2] X. Li, Principles of Fuel Cells, Taylor & Francis, New York, 2005.
[3] L. Carrette, K.A. Friedric, U. Stimming, Fuel Cell 1 (2001) 5.
[4] C.K. Dyer, J. Power Sources 106 (2002) 313.
[5] S.W. Lim, S.W. Kim, H.J. Kim, J.E. Ajn, H.S. Han, Y.G. Shul, J. Power Sources 161 (2006) 27.
[6] F.R. Kalhammer, P.R. Prokopius, V. Roan, G.E. Voecks, Status and Prospects of Fuel Cells as Automobile Engines, Report Prepared for the State of California Air Resources Board, 1998.
[7] R.A.J. Dams, S.C. Moore, P.R. Heyter, Compact Fast Response Methanol Fuel Processing System for PEMFC Electric Vehicles, Fuel Cell Seminar Abstracts, Palm Springs, California, 2000, p. 234.
[8] A.V. Pattekar, M.V. Kothare, S.V. Karnik, M.K. Hatalis, A micro-reactor for in-situ hydrogen production by ctalytic reforming, in: Proceedings of the 5th International Conference on Micro-reaction Technology, Strusbourg, France, 2001.
[9] M. Park, B. Heydorn, Micro-Fuel Cell, A Report from SRI Consulting Business Intelligence, California, 2002.
[10] S. Surampudi, S.R. Narayanan, E. Vamos, H. Frank, G. Halpert, A. LaConti, J. Kosek, G. Prakash, G.A. Olah, J. Power Sources 47 (1994) 377.
[11] A. Kuver, I. Vogel, W. Vielstich, J. Power Sources 52 (1994) 77.
[12] L. Jorisseu, V. Gogel, J. Garchi, J. Power Sources 105 (2002) 267.
[13] W.C. Choi, J.D. Kim, S.I. Woo, J. Power Sources 96 (2001) 411.
[14] S.R. Yoon, C.H. Hwang, W.I. Cho, H.I. Oh, S.A. Hong, H.Y. Ha, J. Power Sources 106 (2002) 215.
[15] H.J. Kim, H.J. Kim, Y.G. Shul, H.S. Han, J. Power Sources 135 (2004) 66.
[16] H.J. Kim, Y.G. Shul, H.S. Han, J. Power Sources 158 (2006) 137.
[17] J. Sank, J. Byun, H. Kim, J. Power Sources 132 (2004) 59.
[18] Z. Florjanczyk, E.W. Barry, Z. Poltarzewski, Solid State Ionics 145 (2001) 119.
[19] S. Ren, G. Sun, C. Li, S. Song, Q. Xin, X. Yang, J. Power Sources 157 (2006) 724.
[20] P. Bebin, M. Caravanier, H. Galiano, J. Membr. Sci. 278 (2006) 35.
[21] A. Sacca, A. Carbone, E. Passalacqua, A. D'Epifano, S. Licoccia, E. Traversa, E. Sala, F. Traini, R. Ornelsas, J. Power Sources 152 (2006) 16.
[22] Y.T. Kim, K.H. Kim, M.K. Song, H.W. Rhee, Curr. Appl. Phys. 6 (2006) 612.
[23] P. Costamagna, C. Yang, A.B. Bocarsly, S. Srinivasan, Electrochim. Acta 47 (2002) 1023.
[24] F. Damay, L.C. Klein, Solid State Ionics 162–163 (2003) 261.
[25] K.Y. Cho, H.Y. Jung, S.S. Shin, N.S. Choi, S.J. Sung, J.K. Park, J.H. Choi, K.W. Park, Y.E. Sung, Electrochim. Acta 50 (2004) 589.
[26] S. Licoccia, E. Traversa, J. Power Sources 159 (2006) 12.